15

MASS TRANSFER IN FLUID SYSTEMS

In Chapters 2 and 7, we demonstrated the development of differential equations pertinent to momentum and energy transport in simple fluid systems. In this chapter, we shall consider how to formulate and describe elementary diffusion and mass transfer problems in fluid systems. We use practically the same procedure in this situation as we did previously; we develop a differential equation, and a solution containing arbitrary constants evolves. These constants are evaluated by applying boundary conditions that specify the concentration or the mass flux at the bounding surfaces. Again, we demonstrate the principles involved by considering specific examples, but first let us reconsider the general situation as outlined in Section 13.2.2.

Species A in a gas stream moving in the x-direction is under the influence of a concentration gradient, also in the x-direction. The molar flux of A relative to stationary coordinates is then made up of two parts: $C_A v_x^*$ which is the molar flux of A resulting from the bulk motion, and $j_{Ax} = -CD_A(\partial X_A/\partial x)$ which is the diffusive contribution. Thus

$$N_{Ax} = -CD_A \frac{\partial X_A}{\partial x} + C_A v_x^* = C_A v_{Ax}. \tag{15.1}$$

Here v_x^* is the local *molar average velocity* in the x-direction, and v_{Ax} is the velocity of A in the x-direction with respect to stationary coordinates, and C is the local total molar concentration in the solution. Thus, we define v_x^* so that the total *molar flux* of all components in the x-direction is made up of the sum of the component fluxes in the same direction:

$$Cv_x^* = \sum_{i=1}^{n} C_i v_{ix}. \tag{15.2}$$

For a binary A–B system, we write

$$v_x^* = \frac{1}{C}\left(C_A v_{Ax} + C_B v_{Bx}\right)$$

$$= \frac{1}{C}\left(N_{Ax} + N_{Bx}\right). \tag{15.3}$$

When we combine Eq. (15.3) with Eq. (15.1), we obtain a form of Fick's first law for a binary solution:

$$N_{Ax} = X_A(N_{Ax} + N_{Bx}) - CD_A \frac{\partial X_A}{\partial x}. \tag{15.4}$$

15.1 DIFFUSION THROUGH A STAGNANT GAS FILM

Consider the system shown in Fig. 15.1 where liquid A is evaporating into gas B, and a constant liquid level at $x = 0$ is maintained. At the liquid–gas phase interface ($x = 0$), the gas phase concentration of A is that corresponding to the vapor pressure of A at that temperature.* For simplicity, also assume that the solubility of B in liquid A is negligible and that the entire system is maintained at a constant temperature and pressure. At the top of the tube, a stream of A–B gas flows past slowly, thereby maintaining a constant concentration of A at $x = l$ which is less than the liquid–gas interface concentration. Therefore, a concentration difference of A exists between $x = 0$ and $x = l$, which causes diffusion. When the system attains a steady state, there is a net motion of A away from the evaporating surface and the vapor B is stationary.

Under these conditions, despite the fact that gas B is stationary, there is bulk motion of fluid since A itself is moving, and its motion contributes to the average velocity. Thus we refer to Eq. (15.4) for the flux of A with $N_{Bx} = 0$. Solving for N_{Ax}, we obtain

$$N_{Ax} = -\frac{CD_A}{1 - X_A}\frac{dX_A}{dx}. \tag{15.5}$$

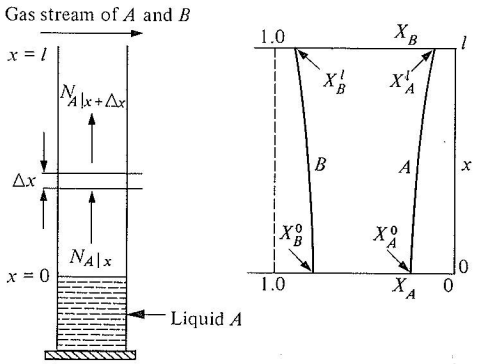

Fig. 15.1 Diffusion of A through B at steady state. B is not in motion, but note that the graph shows how its concentration profile is not linear because of the motion of A.

* This, of course, implies that equilibrium is maintained at the interface, i.e., from a very simplified mechanistic viewpoint, atoms (or molecules) can readily leave the liquid state and enter the gas phase. This assumption is valid except at very high diffusion rates where the rate of transfer of atoms across the liquid–gas interface is not able to keep pace with the exhaustion of the atoms away from the interface.

A mass balance on a unit volume Δx of column height (see Fig. 15.1) for steady state is

$$SN_{Ax}|_x - SN_{Ax}|_{x+\Delta x} = 0, \tag{15.6}$$

in which S is the cross-sectional area. In the expected manner, we divide by Δx and take the limit as $\Delta x \to 0$:

$$\frac{dN_{Ax}}{dx} = 0. \tag{15.7}$$

Substitution of Eq. (15.6) for N_{Ax} yields

$$\frac{d}{dx}\left(\frac{CD_A}{1 - X_A} \cdot \frac{dX_A}{dx}\right) = 0. \tag{15.8}$$

As pointed out in Chapter 13, diffusion coefficients for isothermal gas solutions are very nearly independent of concentration; also, C is constant for an ideal gas mixture at constant temperature and pressure. Hence we simplify the derivative further:

$$\frac{d}{dx}\left(\frac{1}{1 - X_A} \cdot \frac{dX_A}{dx}\right) = 0. \tag{15.9}$$

Two successive integrations can be made directly, resulting in

$$-\ln (1 - X_A) = c_1 x + c_2, \tag{15.10}$$

and we determine the constants by use of the boundary conditions:

$$\text{B.C.1:} \quad \text{at } x = 0, \quad X_A = X_A^0; \tag{15.11a}$$

$$\text{B.C.2:} \quad \text{at } x = l, \quad X_A = X_A^l. \tag{15.11b}$$

When we evaluate the constants and substitute them into Eq. (15.10), we obtain the concentration profile:

$$\ln\left(\frac{1 - X_A}{1 - X_A^0}\right) = \frac{x}{l} \ln\left(\frac{1 - X_A^l}{1 - X_A^0}\right), \tag{15.12}$$

or

$$\ln\left(\frac{X_B}{X_B^0}\right) = \frac{x}{l} \ln\left(\frac{X_B^l}{X_B^0}\right). \tag{15.13}$$

Figure 15.1 shows these solutions, where the slope dX_A/dx is not uniform with x although the flux N_{Ax} is. A gradient of A in the gas must be accompanied by a gradient of B. Consequently, B has a tendency to diffuse down the column, but this diffusive tendency is exactly compensated by the opposing bulk motion of the gas in the direction of diffusion of gas A.

The information that is most often sought after is the rate of mass transfer at the liquid–gas interface. We obtain this by using Eq. (15.5):

$$N_{Ax}|_{x=0} = -\frac{CD_A}{1 - X_A^0}\left(\frac{dX_A}{dx}\right)_{x=0} = \frac{CD_A}{l} \ln\left(\frac{1 - X_A^l}{1 - X_A^0}\right), \tag{15.14}$$

or

$$N_{Ax}|_{x=0} = \frac{CD_A}{(X_B)_{\ln}}\left(\frac{X_A^0 - X_A^l}{l}\right), \tag{15.15}$$

where $(X_B)_{\ln}$ is the *log mean* of the terminal values of X_B.

$$(X_B)_{\ln} = \frac{X_B^l - X_B^0}{\ln (X_B^l/X_B^0)}. \tag{15.16}$$

Equation (15.15) is somewhat more appealing because a characteristic concentration difference $X_A^0 - X_A^l$ over a distance l is evident. For a gas in which species A is dilute, Eq. (15.15) reduces to

$$N_{Ax}|_{x=0} = D_A\left(\frac{C_A^0 - C_A^l}{l}\right), \tag{15.17}$$

which could have resulted from originally ignoring bulk motion and expressing the flux of A simply as

$$j_{Ax} = -D_A \frac{dC_A}{dx}. \tag{15.18}$$

Typical applications of Eqs. (15.14) and (15.15) are evaporation and sublimation processes which involve diffusion of the vapor being created (gas A) through a stationary gas (gas B). Also, a method for measuring diffusion coefficients is to measure the rate of fall of liquid A in a small glass tube as gas B passes over the top. Furthermore, these results find use in the "film theories" of mass transfer.

Example 15.1 In order to determine the diffusivity of Mn in the gas phase, a melt of pure Mn is held in a chamber at 1600°C through which pure Ar flows. The level of the Mn is 2.0 cm below the edge of the crucible. The weight of the crucible is monitored continuously, and when the rate of weight loss is steady with time, that rate is found to be 2.65×10^{-7} mol cm^{-2}-sec^{-1}. Calculate $D_{\text{Mn–Ar}}$.

Solution. At 1600°C, $P_{\text{Mn}}^0 = 0.03$ atm, which may be taken as the pressure just above the liquid surface.

The pressure of manganese may be taken as zero at the crucible edge, as the argon flowing across the opening removes it immediately.

Since the concentration of manganese is clearly dilute, D_{Mn-Ar} is obtained directly from Eq. (15.17). The concentration is expressed in mol cm^{-3}.

$$C_A^0 = \frac{P_A^0}{RT} = \frac{0.03 \text{ atm} \mid \text{mol-°K} \mid 1}{0.08205 \text{ l-atm} \mid 10^3 \text{ cm}^3 \mid 1873\text{°K}}$$

$$= 1.61 \times 10^{-7} \text{ mol cm}^{-3};$$

$$D_{Mn-Ar} = \frac{2.65 \times 10^{-7} \times 2.0}{1.61 \times 10^{-7}} = 3.3 \text{ cm}^2/\text{sec}.$$

15.2 DIFFUSION IN A MOVING GAS STREAM

Figure 15.2 illustrates one technique which we use to determine the vapor pressure of a metal (liquid or solid). Argon, as a carrier gas, passes over the sample which is at the temperature corresponding to the vapor pressure being determined. This gas, containing the saturation concentration of the metal vapor, enters the exit tube at $z = 0$, and at the cool end of the exit tube the metal condenses out and deposits where we can collect it for subsequent mass determination.

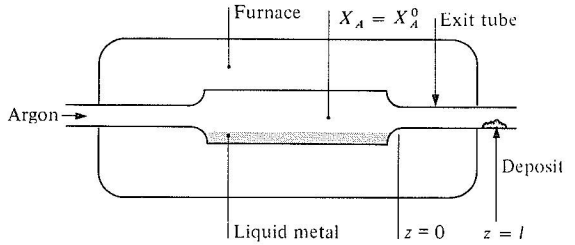

Fig. 15.2 Diffusion in a moving gas stream.

A mass balance applied to a section Δz long for steady state yields

$$\frac{dN_{Az}}{dz} = 0. \tag{15.19}$$

We may choose either Eq. (15.1) or Eq. (15.4) to represent N_{Az}; here we select Eq. (15.1) from which we write

$$v_z^* \frac{dC_A}{dz} - \frac{d}{dz}\left(CD_A \frac{dX_A}{dz}\right) = 0. \tag{15.20}$$

We can certainly consider that the argon–metal gas solution is ideal, and if the temperature variation between $z = 0$ and $z = l$ is small, then C and D_A are constants, and Eq. (15.20) takes the form

$$\frac{d^2X_A}{dz^2} - \frac{v_z^*}{D_A}\frac{dX_A}{dz} = 0. \tag{15.21}$$

The boundary conditions can be represented as:

$$\text{B.C.1:} \quad \text{at } z = 0, \quad X_A = X_A^0 \text{ (saturation value)}, \tag{15.21a}$$

$$\text{B.C.2:} \quad \text{at } z = l, \quad X_A = 0. \tag{15.21b}$$

The second boundary condition implies that the temperature at l is low enough so that the vapor pressure of A is negligible. We can obtain the solution to Eq. (15.21) directly by integrating twice, or by treating it as a linear homogeneous differential equation with constant coefficients. Applying the latter method, the solution is

$$X_A = c_1 e^{r_1 z} + c_2 e^{r_2 z}, \tag{15.22}$$

where r_1 and r_2 are the roots of

$$r^2 - \frac{v_z^*}{D_A} r = 0. \tag{15.23}$$

Thus, $r_1 = 0$ and $r_2 = v_z^*/D_A$, and the solution is

$$X_A = c_1 + c_2 \exp\left(\frac{v_z^*}{D_A} z\right). \tag{15.24}$$

We evaluate the arbitrary constants by using Eqs. (15.24) and (15.21a and b):

$$c_2 = -\frac{X_A^0}{\left[\exp\left(\frac{v_z^* l}{D_A}\right) - 1\right]}, \tag{15.25}$$

and

$$c_1 = X_A^0 \left[1 + \frac{1}{\exp\left(\frac{v_z^* l}{D_A}\right) - 1}\right]. \tag{15.26}$$

The concentration profile can then be written:

$$\frac{X_A}{X_A^0} = \frac{\exp\left(\frac{v_z^* l}{D_A}\right) - \exp\left(\frac{v_z^* z}{D_A}\right)}{\exp\left(\frac{v_z^* l}{D_A}\right) - 1}. \tag{15.27}$$

We evaluate the flux at which the metal vapor enters the exiting gas stream at $z = 0$.

$$N_{Az}|_{z=0} = C\left[-D_A\left(\frac{\partial X_A}{dz}\right)_{z=0} + X_A^0 v_z^*\right],$$

or

$$N_{Az}|_{z=0} = Cv_z^* X_A^0 \left[1 - \frac{1}{1 - \exp\left(\frac{v_z^* l}{D_A}\right)} \right]. \tag{15.28}$$

If S is the cross-sectional area of the tube, then $SN_{Az}|_{z=0}$ represents the amount of A passing through the tube; experimentally, we determine this quantity by weighing the condensate formed at $z = l$ over a measured period of time. The product SCv_z^* is the total molar flow down the tube, and simply represents the number of moles of argon passed per unit time plus the moles of condensate collected per unit time. The vapor pressure of A is related to these experimental quantities by

$$\frac{P_A^0}{P} = X_A^0 = \frac{SN_{Az}|_{z=0}}{SCv_z^*} \left[\frac{\exp\left(\frac{v_z^* l}{D_A}\right) - 1}{\exp\left(\frac{v_z^* l}{D_A}\right)} \right], \tag{15.29}$$

where P_A^0 is the vapor pressure of A, and P is the total pressure. Preferably, the effect of diffusion should be negligible for best experimental results due to the uncertainty of the diffusion coefficient and because we would have to assume an experimental set up that corresponds to the mathematical formulation.

The real value of the analysis lies in the group $v_z^* l/D_A$ which indicates how to set up the experiment, so that the effects of diffusion may be ignored. If $v_z^* l/D_A$ is > 5, the effect of diffusion may be ignored because the last term in Eq. (15.29) is > 0.993 and < 1.0. To insure sufficiently high values of $v_z^* l/D_A$, the experimentalist should provide a small diameter tube between $z = 0$ and $z = l$, and use argon or nitrogen as the carrier gas, rather than hydrogen or helium, since D in the lighter gases is larger than in the heavier gases.

Example 15.2 An experimental apparatus is being constructed to study the thermodynamics of Mn–Cu alloys by measuring the Mn vapor pressure over the molten alloys at 1400°K. In order to use the transport technique, what exit tube dimensions and argon gas flow rates should be used?

Solution. The criterion that provides the most direct experimental measurement of P_{Mn}^0 (the equilibrium pressure over the alloy) is

$$P_{Mn}^0 = P \frac{N_{Mn}}{N},$$

where N_{Mn} is the number of moles of Mn condensed out and $N = N_{Mn} + N_{Ar}$ = total moles of gas passing through the exit tube over some period of time. This is essentially true when $v^* l/D_{Mn-Ar} \geq 5.0$.

We evaluate D_{Mn-Ar} at 1400°K as 2.6 cm^2-sec^{-1}. Therefore, $v^* l$ must be greater than 13.0 cm^2-sec^{-1}. Since $v^* \cong 4\dot{n}RT/\pi d^2 P$, and $\dot{n} \cong \dot{n}_{Ar}$ (mol Ar sec^{-1}), then

$$\frac{4\dot{n}_{Ar} RTl}{\pi P} \geq 13.0 d^2.$$

The figure below shows the results, with the preferred design being to the right-hand side of each curve.

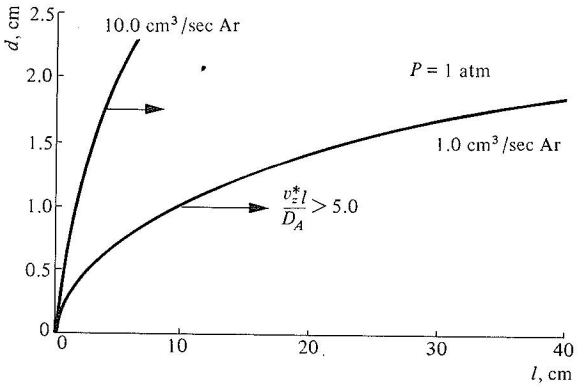

At temperatures where P_{Mn}^0 is greater than negligible values, and $\dot{n} > \dot{n}_{Ar}$, the curves should be shifted even further to the right for better results.

15.3 DIFFUSION INTO A FALLING LIQUID FILM

In this section, we shall consider a fluid system moving in such a way that the velocity distribution is unaffected by diffusion into the fluid. Figure 15.3 shows a film of liquid B falling in laminar flow down a wall. Gas A is absorbed at the liquid–gas interface; we shall restrict the situation to that where the penetration distance of A into B is small relatively to the film thickness. We wish to calculate the amount of gas absorbed after the film travels a distance L.

First, we develop a mass balance on component A. The gas–liquid interface concentration of A at all points along the film, is the saturation value C_A^0; thus A diffuses into the liquid which initially contains less than the saturation amount of A. As the film drops, the liquid is exposed to C_A^0 for a longer time and more penetration of A into the film results. We see, therefore, that C_A changes both with x and z, and we select the unit volume: Δx by Δz by unity in the y-direction.

Then the mass balance for A is simply

$$N_{Az}|_z \cdot \Delta x - N_{Az}|_{z+\Delta z} \cdot \Delta x + N_{Ax}|_x \cdot \Delta z - N_{Ax}|_{x+\Delta x} \cdot \Delta z = 0. \tag{15.30}$$

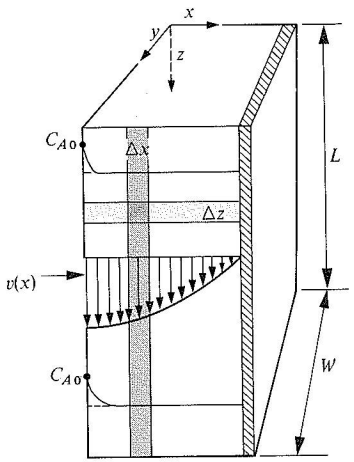

Fig. 15.3 Absorption into a falling film.

Dividing by $\Delta x \Delta z$, and performing the usual limiting process, we get

$$\frac{\partial N_{Az}}{\partial z} + \frac{\partial N_{Ax}}{\partial x} = 0. \tag{15.31}$$

We now have to insert into this equation the expressions for N_{Az} and N_{Ax}. For the molar flux in the z-direction, we write

$$N_{Az} = -CD_A \frac{\partial X_A}{\partial z} + C_A v_z^*, \tag{15.32}$$

and neglect the diffusive contribution, realizing that A moves in the z-direction primarily due to bulk flow. In addition, for small increases in the concentration of A, $v_z^* \cong v_z$. Finally, we give N_{Az} by the simplified expression

$$N_{Az} = C_A v_z. \tag{15.33}$$

For the molar flux in the x-direction, we write

$$N_{Ax} = -D_A \frac{\partial C_A}{\partial x} + C_A v_x^*. \tag{15.34}$$

That is, in the x-direction, A is transported primarily by diffusion, there being almost no bulk flow in the x-direction due to the small solubility of A in B. Substitution of Eqs. (15.32) and (15.34) into Eq. (15.31) yields the differential equation for $C_A(x, z)$:

$$v_z \frac{\partial C_A}{\partial z} = D_A \frac{\partial^2 C_A}{\partial x^2}. \tag{15.35}$$

When dealing with energy transport in a convective system, it is necessary to obtain the velocity profile $v_z(x)$; similarly, we need to describe the velocity for the analogous situation of mass transfer in a convective system. For a falling film, we have already worked this out in Chapter 2 in the absence of mass transfer at the fluid surface, and we know that the results for fully developed flow are

$$v_z = v_{\max}\left[1 - \left(\frac{x}{\delta}\right)^2\right],$$

where δ is the film thickness, and x is the distance into the film from the gas–liquid surface.

If, as indicated in Fig. 15.3, A has penetrated only a slight distance into the film, then for the most part species A sees only $v_{\max}$. Further, since it does not penetrate very far, we can consider that the liquid is semi-infinite. These conditions would hold, for example, for short contact times. With these approximations we write the differential equation and the boundary conditions:

$$v_{\max} \frac{\partial C_A}{\partial z} \cong D_A \frac{\partial^2 C_A}{\partial x^2}. \tag{15.36}$$

$$\text{At } z = 0, \qquad C_A = C_A^i, \qquad x \geq 0, \tag{15.37a}$$

$$\text{at } x = 0, \qquad C_A = C_A^0, \qquad L \geq z \geq 0, \tag{15.37b}$$

$$\text{at } x = \infty, \qquad C_A = C_A^i, \qquad L \geq z \geq 0. \tag{15.37c}$$

Note that we may alternatively view $z/v_{\max}$ as the time t, over which a moving slice of liquid has been subjected to the surface concentration C_A^0. Thus, we recognize the solution to Eq. (15.36), subject to Eqs. (15.37a), (15.37b), and (15.37c), as the solution for the temperature distribution in a semi-finite solid, initially at a uniform temperature, which is suddenly subjected to a new constant surface temperature. Then, referring to Eq. (9.110), we have

$$\frac{C_A - C_A^0}{C_A^i - C_A^0} = \operatorname{erf} \frac{x}{2\sqrt{D_A z / v_{\max}}}. \tag{15.38}$$

Now knowing the concentration profile, we proceed to determine the local diffusion mass flux at the surface, $x = 0$:

$$N_{Ax}|_{x=0} = -D_A \left(\frac{\partial C_A}{\partial x}\right)_{x=0} = (C_A^0 - C_A^i)\sqrt{\frac{D_A v_{\max}}{\pi z}}, \tag{15.39}$$

the average rate of A transferred per unit across the entire surface between $z = 0$ and $z = L$ being

$$\bar{N}_{Ax}|_{x=0} = \frac{1}{L}\int_0^L N_{Ax}|_{x=0}\,dz$$

$$= 2(C_A^0 - C_A^i)\sqrt{\frac{D_A v_{\max}}{\pi L}}. \tag{15.40}$$

Pigford[1] solved the complete equation

$$v_{\max}\left[1 - \left(\frac{x}{\delta}\right)^2\right]\frac{\partial C_A}{\partial z} = D_A\frac{\partial^2 C_A}{\partial x^2}, \tag{15.41}$$

and obtained the result:

$$\frac{\bar{C}_A^L - C_A^0}{C_A^i - C_A^0} = 0.7857e^{-5.1213\eta} + 0.1001e^{-39.318\eta} + \cdots, \tag{15.42}$$

where $\eta = D_A L/\delta^2 v_{\max}$, and $\bar{C}_A^L$ = bulk average composition of the liquid at L.

For small values of η, corresponding to short contact times or very thick films, we obtain

$$\frac{\bar{C}_A^L - C_A^0}{C_A^i - C_A^0} = \sqrt{\frac{6}{\pi}}\sqrt{\frac{D_A L}{\delta^2 \bar{V}}}, \tag{15.43}$$

and for long times, we have

$$\frac{\bar{C}_A^L - C_A^0}{C_A^i - C_A^0} = 0.7857e^{-5.1213\eta}. \tag{15.44}$$

15.4 THE MASS-TRANSFER COEFFICIENT

In Chapter 7, we analyzed simple problems of heat transfer with laminar convection, and formulated the temperature distribution from which we calculated heat-transfer rates by evaluating the heat fluxes at the fluid–solid boundary. With the fluxes, we wrote expressions for the heat-transfer coefficients, and we saw that $\mathrm{Nu} = f(\mathrm{Re}, \mathrm{Pr})$, and gained insight into what was to follow in Chapter 8 where we presented the correlations for heat transfer in turbulent convective systems.

Having considered diffusion in the presence of forced convection in Section 15.3, it is convenient to introduce the *mass-transfer coefficient*. As we have mentioned, we may treat the movement of a species as the sum of a diffusional contribution and a bulk flow contribution (see Eq. 15.1). To be analogous with heat transfer, a mass-transfer coefficient for transfer of A into or out of a phase is defined in terms of the *diffusive* contribution normal to the interface:

$$k_M = \frac{j_A^0}{C_A^0 - C_{A\infty}} = -\frac{D_A(\partial C_A/\partial x)_{x=0}}{C_A^0 - C_{A\infty}}. \tag{15.45}$$

Here, the superscript 0 refers to quantities evaluated at the interface, and $C_{A\infty}$ to some concentration of A within the fluid, usually the bulk concentration. Note that, while k_M in Eq. (15.45) is defined in terms of the diffusion flux at the surface, in general, at interfaces involving a fluid phase, there is the additional contribution to mass transfer caused by bulk flow. We define the mass-transfer coefficient here only in terms of the diffusive contribution, rather than of the total flux N_A^0. This is because the coefficient so defined is somewhat more fundamental, since we might expect the diffusion flux to be approximately proportional to a characteristic concentration difference as indicated by Eq. (15.45), whereas the bulk flow contribution can be relatively independent of any concentration difference. Similarly, when both heat and mass transfer occur, it is advantageous to retain the definition of the heat-transfer coefficient given by Eq. (8.1), which considers only the conduction flux.

In the limit of low mass-transfer rates, as is often the case, we may neglect the distortion of the velocity and concentration profiles by mass transfer, and the bulk flow term is negligible. Then

$$k_M = \frac{N_A^0}{C_A^0 - C_{A\infty}}. \tag{15.46}$$

This equation is definitional only, and we must evaluate it by means of various analytical expressions for the flux. As the first example of applying Eq. (15.46), consider the results of diffusion into a falling film in Section 15.3. We evaluate the *local* mass-transfer coefficient relating the rate of mass transfer of A into the liquid when the time of contact is short, by substituting Eq. (15.39) into Eq. (15.46).

$$k_{M,z} = \frac{N_{Ax}|_{x=0}}{C_A^0 - C_{A\infty}} = \sqrt{\frac{D_A v_{\max}}{\pi z}}, \tag{15.47}$$

or in terms of dimensionless groups, and recalling that $v_{\max} = \frac{3}{2}\bar{V}$,

$$\frac{k_{M,z}z}{D_A} = \sqrt{\frac{3}{2\pi}}\sqrt{\frac{\bar{V}z}{\nu}}\sqrt{\frac{\nu}{D_A}}. \tag{15.48}$$

The group $k_{M,z}z/D_A$ is called the *Sherwood number*, Sh, or alternatively the *mass transfer Nusselt number*, Nu_M. The Reynolds number should be easily recognized. The Schmidt number, Sc, which is defined by

$$\mathrm{Sc} = \frac{\nu}{D}, \tag{15.49}$$

[1] R. L. Pigford, *Ph.D. Thesis*, University of Illinois, 1941.

is the analog of the Prandtl number encountered in heat transfer. Most available forced-convection mass-transfer correlations are in the form

$$\mathrm{Sh} = f(\mathrm{Re}, \mathrm{Sc}, \text{geometry}),* \tag{15.50}$$

as, for example, in the situation above. Specifically, we could write Eq. (15.48) as

$$\mathrm{Sh}_z = \sqrt{\frac{3}{2\pi}}\,\mathrm{Re}_z^{1/2}\mathrm{Sc}^{1/2}. \tag{15.51}$$

In this case, by subscripting with z, we emphasize that local values are being considered. If we used Eq. (15.40) instead of Eq. (15.39), we would define an *average* mass-transfer coefficient over the film length L.

$$k_M = \frac{(C_A^0 - C_A^i)\left(\dfrac{4D_A v_{\max}}{\pi L}\right)^{1/2}}{(C_A^0 - C_A^i)} = \sqrt{\frac{6D_A\bar{V}}{\pi L}}. \tag{15.52}$$

We can then write this as

$$\frac{k_M L}{D_A} = \sqrt{\frac{6}{\pi}}\sqrt{\frac{\bar{V}L}{\nu}}\sqrt{\frac{\nu}{D_A}},$$

or in dimensionless form

$$\mathrm{Sh}_L = \sqrt{\frac{6}{\pi}}\,\mathrm{Re}_L^{1/2}\mathrm{Sc}^{1/2}, \tag{15.53}$$

where the subscript L indicates that the quantities are averaged over the entire film length.

In the case of long contact times, where Eq. (15.44) applies, the rate at which A is absorbed in the distance dz is

$$\bar{V}\delta\, d\bar{C}_A = k_M(C_A^0 - \bar{C}_A)\, dz.$$

Over the entire length of the film, the absorption rate of A is

$$\bar{V}\delta \int_{C_A^i}^{\bar{C}_A^L} \frac{d\bar{C}_A}{C_A^0 - \bar{C}_A} = k_M \int_0^L dz.$$

The integration yields

$$k_M = \frac{\bar{V}\delta}{L} \ln \frac{C_A^0 - C_A^i}{C_A^0 - \bar{C}_A^L}. \tag{15.54}$$

* The product ReSc which we often encounter in the literature on mass transfer, is sometimes called the Peclet number, Pe.

Substituting Eq. (15.44), we obtain

$$k_M = \frac{\bar{V}\delta}{L}\,[\ln(e^{5.1213\eta} - \ln 0.7857)]$$

$$= \frac{\bar{V}\delta}{L}\,[5.1213\eta + 0.241]$$

$$\cong 3.42\frac{D_A}{\delta}. \tag{15.55}$$

By rearranging this expression, we get

$$\frac{k_M\delta}{D_A} = \mathrm{Sh} \cong 3.42, \tag{15.56}$$

which is similar to the results given in Table 7.1 where the Nusselt number was found to be a constant for fully developed laminar flow. We consider that this equation is applicable at $\mathrm{Re}\,(= \Gamma/\eta) \leq 25$, where Γ is the mass flow rate per unit width of film.

Having been tested for absorption of gases into liquids flowing down wetted-wall columns, Eq. (15.56) has been found to somewhat underestimate the actual mass-transfer coefficient. At low Reynolds numbers, this is now understood to be partly due to the so-called *Marangoni effect*, in which upward-directed surface tension forces counteract the downward-directed gravitational forces, causing rippling and turbulence on the surface and an increase in transfer which is not anticipated in the simplified development described above.

Example 15.3 A method for degassing molten metals involves exposing a thin film of metal to vacuum by allowing it to flow continuously over an inclined plate. Calculate the average hydrogen concentration of a ferrous alloy with an initial concentration of 1 cm^3 H_2 (STP) per cm^3 of alloy flowing down a plate 100 cm long and 15 cm wide, which is inclined at an angle of 1 deg from the horizontal. The concentration of hydrogen at the surface exposed to the vacuum may be taken as zero. The desired film thickness is 1 mm. Data are as follows: $\rho = 8.32\ \mathrm{g/cm}^3$, $\eta = 6$ cP, $D_H = 1.3 \times 10^{-4}\ \mathrm{cm}^2/\mathrm{sec}$.

Solution. Using Eq. (2.14), we find the average velocity:

$$\bar{V} = \frac{(8.32\ \mathrm{g/cm}^3)(980\ \mathrm{cm/sec}^2)\,(0.1\ \mathrm{cm})^2(\cos 89°)}{3(6 \times 10^{-2}\ \mathrm{g/cm\text{-}sec})} = 7.90\ \mathrm{cm/sec}.$$

The contact time is

$$\frac{L}{\bar{V}} = \frac{100\ \mathrm{cm}}{7.90\ \mathrm{cm/sec}} = 12.7\ \mathrm{sec}.$$

Since this is very short, we make use of Eq. (15.52) to calculate an average k_M:

$$k_M = \sqrt{\frac{6D_H\bar{V}}{\pi L}} = \sqrt{\frac{(6)(1.3 \times 15^4)(7.9)}{(3.14)(100)}}$$

$$= 1.71 \times 10^{-3} \text{ cm/sec.}$$

Then

$j_{H_2} = (1.71 \times 10^{-3} \text{ cm/sec})(1 \text{ cm}^3 \text{ H}_2/\text{cm}^3 \text{ alloy}) = 1.71 \times 10^{-3} \text{ cm}^3 \text{ H}_2/\text{cm}^2\text{-sec}$

Total content removed per cm^2 of exposed surface is $= j_{H_2}$ (contact time)

$= 2.16 \times 10^{-2} \text{ cm}^3 \text{ H}_2/\text{cm}^2$ film.

Initial total content $= (1 \text{ cm}^3 \text{ H}_2/\text{cm}^3 \text{ alloy}) \cdot (0.1 \text{ cm}^3 \text{ alloy}/\text{cm}^2 \text{ film})$

$= 0.1 \text{ cm}^3 \text{ H}_2/\text{cm}^2$ film.

Final total content $= 0.1000 - 0.0216 = 0.0784 \text{ cm}^3 \text{ H}_2/\text{cm}^2$ film, or the average content of the metal is reduced to $0.784 \text{ cm}^3 \text{ H}_2/\text{cm}^3$ alloy.

Under many circumstances encountered in interphase mass transfer, the bulk flow term is not important, and the diffusive contribution in the mass flux equation is all that we need to consider. On the other hand, there may be occasions, particularly where transfer to and from gas phases is involved, in which this contribution is not negligible. In this case, we write

$$N_A = \theta k_M (C_A^0 - C_A^i), \tag{15.57}$$

where N_A is the total interphase flux, and θ is a correction factor that depends on N_A, N_B, and k_M according to

$$\theta = \frac{N_A + N_B}{k_M\left[\exp\left(\frac{N_A + N_B}{k_M}\right) + 1\right]}. \tag{15.58}$$

Figure 15.4 gives a graph of θ as a function of $(N_A + N_B)/k_M = \phi$. A limiting case is equimolar counter-diffusion, in which $N_A = -N_B$ and $\phi = 0$, so that $\theta = 1.0$ and no correction is involved.

In case we do not know N_A, and $N_B = 0$, the expression

$$1 + \frac{C_A^0 - C_A^i}{\frac{N_A}{N_A + N_B} - C_A^0} = \exp\left(\frac{N_A + N_B}{k_M}\right) \tag{15.59}$$

may be used to evaluate N_A at high mass-transfer rates.

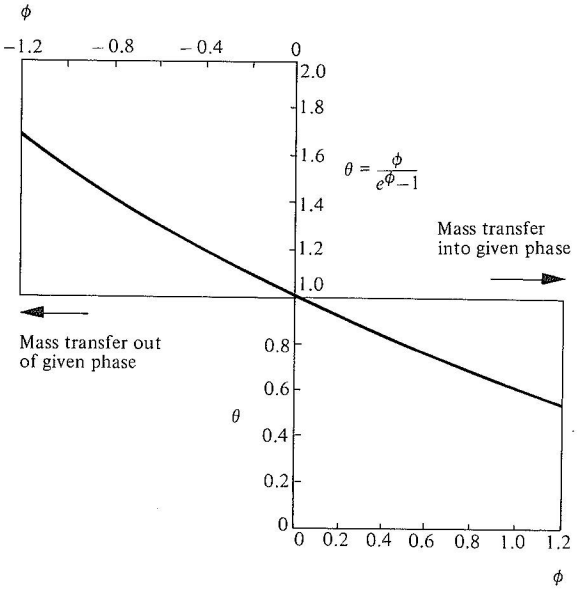

Fig. 15.4 The variation of coefficients with mass transfer rate. (From R. B. Bird, W. E. Stewart, and E. N. Lightfoot, *Transport Phenomena*, Wiley, New York, 1960, page 664.)

Thus, forced convection mass transfer at high mass-transfer rates (large N_A and/or N_B) is generally correlated by

$$\text{Sh} = f(\text{Re}, \text{Sc}, N_A, \text{and geometry}). \tag{15.60}$$

For the most part, we shall not make use of this latter form.

15.5 FORCED CONVECTION OVER A FLAT PLATE—APPROXIMATE INTEGRAL TECHNIQUE

In Chapters 2 and 7, we developed expressions for the thickness of a momentum boundary layer and a thermal boundary layer of a fluid flowing past a plate. In this section, we shall again apply the approximate integral technique to obtain a solution for the thickness of a concentration boundary layer developing as a component diffuses from the solid plate into the fluid.

As in Section 7.2.2, consider the process of transfer of A from the solid (pure A) into the fluid (B). We disregard diffusion in the x-direction, it being negligible with respect to the velocity component of mass-transfer in the x-direction. Figure 15.5 depicts the unit volume to which we apply the integral mass balance.

The amount of A flowing into the element is

$$W_{A,x} = \int_0^t C_A v_x \, dy, \tag{15.61}$$

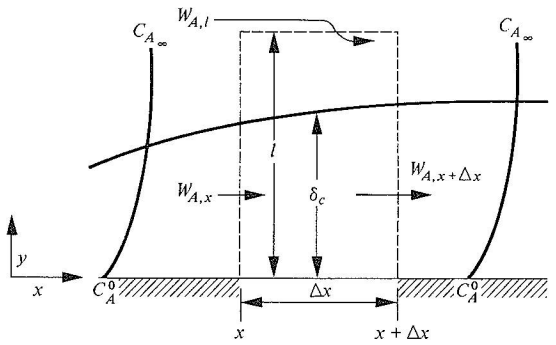

Fig. 15.5 Integrated convective contributions to the concentration boundary layer over a flat plate.

and the amount leaving is

$$W_{A,x+\Delta x} = W_{A,x} + \frac{d}{dx}\left(\int_0^l C_A v_x \, dy\right)\Delta x. \tag{15.62}$$

To satisfy continuity, there is also fluid entering at $y = l$; this amount is

$$W_{A,l} = \frac{d}{dx}\left(C_{A\infty}\int_0^l v_x \, dy\right)\Delta x. \tag{15.63}$$

The mass transfer into the unit element across the phase boundary at $y = 0$ is

$$j_{Ay}|_{y=0}\,\Delta x = -D_A\left(\frac{\partial C_A}{\partial y}\right)_{y=0}\Delta x. \tag{15.64}$$

We now formulate the mass balance for component A:

$$j_{Ay}|_{y=0}\,\Delta x + W_{A,x} + W_{A,l} = W_{A,x+\Delta x}. \tag{15.65}$$

Substituting Eqs. (15.61)–(15.64) into Eq. (15.65) yields

$$-D_A\left(\frac{\partial C_A}{\partial y}\right)_{y=0} = \frac{d}{dx}\left(\int_0^l C_A v_x \, dy - C_{A\infty}\int_0^l v_x \, dy\right). \tag{15.66}$$

The integrals in Eq. (15.66) are split, that is,

$$\int_0^l = \int_0^{\delta_c} + \int_{\delta_c}^l .$$

and then by simplifying, we arrive at

$$D_A\left(\frac{\partial C_A}{\partial y}\right)_{y=0} = \frac{d}{dx}\left[\int_0^{\delta_c}(C_{A\infty} - C_A)v_x \, dy\right]. \tag{15.67}$$

Equation (15.67) is an exact analog of Eq. (7.36). If we assume a concentration profile analogous to Eq. (7.37), that is,

$$\frac{C_A - C_A^0}{C_{A\infty} - C_A^0} = \frac{3}{2}\left(\frac{y}{\delta_c}\right) - \frac{1}{2}\left(\frac{y}{\delta_c}\right)^3, \tag{15.68}$$

which satisfies the conditions

$$\text{B.C.1:} \quad \text{at } y = 0, \quad C_A = C_A^0, \tag{15.69a}$$

$$\text{B.C.2:} \quad \text{at } y = \delta_c, \quad C_A = C_{A\infty}, \tag{15.69b}$$

then by substituting the assumed velocity distribution, Eq. (2.105), and the concentration distribution, Eq. (15.68), into Eq. (15.67), and following the procedure outlined previously for developing Eq. (7.42), we obtain the expression for the ratio of boundary layers:

$$\frac{\delta_c}{\delta} = \frac{1}{1.026\sqrt[3]{\text{Sc}}}. \tag{15.70}$$

Using Eq. (15.68), the local mass-transfer coefficient is

$$k_{M,x} = \frac{-D_A\left(\frac{\partial C_A}{\partial y}\right)_{y=0}}{C_A^0 - C_{A\infty}} = \frac{3}{2}\frac{D_A}{\delta_c}. \tag{15.71}$$

Thus, we combine Eqs. (15.70), (2.107), and (15.71) to obtain

$$\text{Sh}_x = 0.323\sqrt[3]{\text{Sc}}\sqrt{\text{Re}_x}. \tag{15.72}$$

These solutions are valid for most fluids, including liquid metals, because $(\delta_c/\delta) \ll 1$ for metals. Table 15.1 gives typical magnitudes of Schmidt numbers for fluids.

Table 15.1 Typical magnitudes of Prandtl numbers and Schmidt numbers

	Pr	Sc
Gases	0.6–1.0	0.1–2.0
Liquids	1–10	10^2–10^3
Liquid metals	10^{-2}	10^3

The average mass-transfer coefficient for transfer from a flat plate to a fluid is given by

$$k_M = \frac{1}{L}\int_0^L k_{M,x}\,dx = 0.646\frac{D_A}{L}\mathrm{Sc}^{1/3}\mathrm{Re}_L^{1/2}, \tag{15.73}$$

or

$$\mathrm{Sh}_L = 0.646\,\mathrm{Sc}^{1/3}\mathrm{Re}_L^{1/2}. \tag{15.74}$$

According to Eq. (15.70), the concentration boundary layer and velocity layers for gases are about the same as in heat transfer, where δ_T and δ were similar because Pr was about unity. For liquid metals, however, while we found that in the case of heat transfer $\delta_T \gg \delta$, now we see that $\delta_c \ll \delta$. This means that we can use temperature profiles to predict mass-transfer profiles and rates, or vice versa, for gas phase transfer, but we cannot do likewise for liquid metals, because their concentration and temperature boundary layer profiles differ widely.

The *exact solution* of the problem of describing mass transfer in the above system requires simultaneous solution of the equations of momentum and continuity for both the total material flux and each individual component. We shall discuss the results of such a study in Section 15.7.

15.6 GENERAL EQUATION OF DIFFUSION WITH CONVECTION

In this section, we summarize the general approach to the law of mass conservation in the volume element $\Delta x\,\Delta y\,\Delta z$, depicted in Fig. 2.4, through which a fluid containing A in solution is flowing. In the following expressions, ρ_A is the mass *concentration* (for example, g of A/cm^3 of total solution) as defined by Eq. (13.1). W_{Ax} is the total *mass* flux of A in the x-direction and is composed of a diffusive term and a convective term. Specifically

$$W_{Ax} = -\rho D_A\left(\frac{\partial \rho_A^*}{\partial x}\right) + \rho_A v_x = \rho_A v_{Ax}, \tag{15.75}$$

where ρ is the density of the entire solution, ρ_A^* is the mass *fraction* of A, and v_x is the local *mass average velocity* in the x-direction; thus, we define v_x such that the total mass flux of all components in the x-direction is made up of the sum of the n component fluxes in the same direction:

$$\rho v_x = \sum_{i=1}^{n} \rho_i v_{ix}. \tag{15.76}$$

For a binary, in order to illustrate, we write

$$v_x = \frac{1}{\rho}(\rho_A v_{Ax} + \rho_B v_{Bx})$$

$$= \frac{1}{\rho}(W_{Ax} + W_{Bx}).$$

Now we can proceed to develop a mass balance for the volume element. The various contributions to the mass balance of component A are

Accumulation of mass of A in the volume element	$\Delta x\,\Delta y\,\Delta z\dfrac{\partial \rho_A}{\partial t}$,
Input of A across face at x	$\Delta y\,\Delta z\,W_{Ax}\vert_x$,
Output of A across face at $x + \Delta x$	$\Delta y\,\Delta z\,W_{Ax}\vert_{x+\Delta x}$.

There are also input and output terms in the y- and z-directions. When we write the entire mass balance for species A, divide through by $\Delta x\,\Delta y\,\Delta z$, and take the limits in the usual manner, we obtain the *general equation of continuity for component A*:

$$\frac{\partial \rho_A}{\partial t} + \frac{\partial W_{Ax}}{\partial x} + \frac{\partial W_{Ay}}{\partial y} + \frac{\partial W_{Az}}{\partial z} = 0. \tag{15.77}$$

The quantities W_{Ax}, W_{Ay}, W_{Az} are the rectangular components of the *mass flux vector*, $\boldsymbol{W}_A = \rho_A \boldsymbol{v}_A$, which includes motion of A due to diffusion and bulk flow:

$$\boldsymbol{W}_A = -\rho D_A \nabla \rho_A^* + \rho_A \boldsymbol{v} = \rho_A \boldsymbol{v}_A. \tag{15.78}$$

Finally, by combining Eqs. (15.77) and (15.78), we develop the *diffusion equation* for component A:

$$\frac{\partial \rho_A}{\partial t} + \nabla \cdot \rho_A \boldsymbol{v} = \nabla \cdot \rho D_A \nabla \rho_A^*. \tag{15.79}$$

As is usually the case, simplifications are utilized more frequently than general equations. Often, one can assume constant mass density and D_A, and make some simplification. For *constant* ρ *and* D_A, Eq. (15.79) becomes

$$\frac{\partial \rho_A}{\partial t} + \boldsymbol{v}\nabla \rho_A = D_A \nabla^2 \rho_A, \tag{15.80}$$

or if divided by M_A (molecular weight of A), we get

$$\frac{\partial C_A}{\partial t} + \boldsymbol{v}\nabla C_A = D_A \nabla^2 C_A. \tag{15.81}$$

The left-hand side of this equation is DC_A/Dt, showing direct similarity with Eq. (7.90) which is the basis for the numerous analogies between heat and mass transport in fluids with constant ρ.

The above analysis could have been made equally well in terms of molar fluxes such as we have used previously.

Equation of continuity for component A:

$$\frac{\partial C_A}{\partial t} + (\nabla \boldsymbol{N}_A) = 0. \tag{15.82}$$

Diffusion equation for A in solution:

$$\frac{\partial C_A}{\partial t} + \nabla \cdot C_A \boldsymbol{v}^* = \nabla \cdot C D_A \nabla X_A. \tag{15.83}$$

Table 15.2 The equation of continuity of A in various coordinate systems

Rectangular coordinates:

$$\frac{\partial C_A}{\partial t} + \left(\frac{\partial N_{Ax}}{\partial x} + \frac{\partial N_{Ay}}{\partial y} + \frac{\partial N_{Az}}{\partial z}\right) = 0 \tag{A}$$

Cylindrical coordinates:

$$\frac{\partial C_A}{\partial t} + \left(\frac{1}{r}\frac{\partial}{\partial r}(rN_{Ar}) + \frac{1}{r}\frac{\partial N_{A\theta}}{\partial \theta} + \frac{\partial N_{Az}}{\partial z}\right) = 0 \tag{B}$$

Spherical coordinates:

$$\frac{\partial C_A}{\partial t} + \left(\frac{1}{r^2}\frac{\partial}{\partial r}(r^2 N_{Ar}) + \frac{1}{r\sin\theta}\frac{\partial}{\partial \theta}(N_{A\theta}\sin\theta) + \frac{1}{r\sin\theta}\frac{\partial N_{A\phi}}{\partial \phi}\right) = 0 \tag{C}$$

Table 15.3 The equation of diffusion of A for constant ρ and D_A

Rectangular coordinates:

$$\frac{\partial C_A}{\partial t} + \left(v_x\frac{\partial C_A}{\partial x} + v_y\frac{\partial C_A}{\partial y} + v_z\frac{\partial C_A}{\partial z}\right) = D_A\left(\frac{\partial^2 C_A}{\partial x^2} + \frac{\partial^2 C_A}{\partial y^2} + \frac{\partial^2 C_A}{\partial z^2}\right) \tag{A}$$

Cylindrical coordinates:

$$\frac{\partial C_A}{\partial t} + \left(v_r\frac{\partial C_A}{\partial r} + v_0\frac{1}{r}\frac{\partial C_A}{\partial \theta} + v_z\frac{\partial C_A}{\partial z}\right) = D_A\left(\frac{1}{r}\frac{\partial}{\partial r}\left(r\frac{\partial C_A}{\partial r}\right) + \frac{1}{r^2}\frac{\partial^2 C_A}{\partial \theta^2} + \frac{\partial^2 C_A}{\partial z^2}\right) \tag{B}$$

Spherical coordinates:

$$\frac{\partial C_A}{\partial t} + \left(v_r\frac{\partial C_A}{\partial r} + v_\theta\frac{1}{r}\frac{\partial C_A}{\partial \theta} + v_\phi\frac{1}{r\sin\theta}\frac{\partial C_A}{\partial \phi}\right) = D_A\left(\frac{1}{r^2}\frac{\partial}{\partial r}\left(r^2\frac{\partial C_A}{\partial r}\right) + \frac{1}{r^2\sin\theta}\frac{\partial}{\partial \theta}\left(\sin\theta\frac{\partial C_A}{\partial \theta}\right) + \frac{1}{r^2\sin^2\theta}\frac{\partial^2 C_A}{\partial \phi^2}\right) \tag{C}$$

For constant C and D_A, Eq. (15.83) takes the form

$$\frac{\partial C_A}{\partial t} + \boldsymbol{v}^* \nabla C_A = D_A \nabla^2 C_A. \tag{15.84}$$

This equation is usually applied to low-density gases at constant temperature and pressure. The left-hand side of this equation cannot be written as DC_A/Dt because of the appearance of $\boldsymbol{v}^*$ rather than of $\boldsymbol{v}$. A more simplified form of the above equations, which is used for diffusion in solids or stationary liquids ($\boldsymbol{v} = 0$ in Eq. 15.81), or for equimolar counterdiffusion in gases ($\boldsymbol{v}^* = 0$ in Eq. 15.84), is *Fick's second law of diffusion*:

$$\frac{\partial C_A}{\partial t} = D_A \nabla^2 C_A. \tag{15.85}$$

In Tables 15.2 and 15.3, we summarize the most important equations of this discussion in rectangular, cylindrical, and spherical coordinates. Fick's second law of diffusion can be obtained by setting the velocity components in Table 15.3 equal to zero.

15.7 FORCED CONVECTION OVER A FLAT PLATE—EXACT SOLUTION

As an application of the above equations, consider the flow system discussed in Section 15.5. A thin, semi-infinite plate of solid A dissolves very slowly under steady-state conditions, into an unbounded fluid stream of A and B. The flow is initially at uniform velocity, concentration, and temperature. For constant properties of the fluid, we may write the boundary layer equations of momentum, energy, mass, and continuity:

$$\text{Continuity,} \quad \frac{\partial v_x}{\partial x} + \frac{\partial v_y}{\partial y} = 0, \tag{15.86}$$

$$\text{Momentum,} \quad v_x\frac{\partial v_x}{\partial x} + v_y\frac{\partial v_x}{\partial y} = \nu\frac{\partial^2 v_x}{\partial y^2}, \tag{15.87}$$

$$\text{Energy,} \quad v_x\frac{\partial T}{\partial x} + v_y\frac{\partial T}{\partial y} = \alpha\frac{\partial^2 T}{\partial y^2}, \tag{15.88}$$

$$\text{Mass,} \quad v_x\frac{\partial C_A}{\partial x} + v_y\frac{\partial C_A}{\partial y} = D_A\frac{\partial^2 C_A}{\partial y^2}. \tag{15.89}$$

Equations (15.86)–(15.88) were obtained in Chapter 7 for zero mass transfer. The assumption that the same equations are valid in the presence of mass transfer means that any additional momentum and energy fluxes associated with mass transfer are negligible. Equation (15.89) is derived from Eq. (A) in Table 15.3 with $\partial C_A/\partial t = 0$, $\partial^2 C_A/\partial z^2 = 0$, $v_z = 0$, and by neglecting the negligible amount of diffusion in the x-direction.

A typical set of boundary conditions that may be specified is:

$$\text{B.C. 1:} \quad x \le 0, \quad v_x = V_\infty, \quad v_y = 0, \quad T = T_\infty, \quad C_A = C_{A\infty} \quad \text{for all } y, \tag{15.90a}$$

$$\text{B.C. 2:} \quad y = \infty, \quad v_x = V_\infty, \quad v_y = 0, \quad T = T_\infty, \quad C_A = C_{A\infty} \quad \text{for } x > 0, \tag{15.90b}$$

$$\text{B.C. 3:} \quad y = 0, \quad v_x = 0, \quad v_y = v_0, \quad T = T_0, \quad C_A = C_A^0 \quad \text{for } x > 0. \tag{15.90c}$$

The fact that $v_y = v_0$ at the wall accounts for the bulk motion accompanying diffusion from the wall. The method of solving Eqs. (15.86)–(15.89) subject to the conditions (Eqs. 15.90 a, b, and c) is not given here, but Fig. 15.6 presents the results for certain values of Pr and Sc. Note that the differential equations and boundary conditions for temperature and concentration are analogous; therefore, when Pr = Sc = 1, the velocity, temperature, and concentration profiles within the boundary layer must coincide. Figure 15.6 shows these results, along with the results for Pr = Sc = 0.7; velocity profiles remain unchanged.

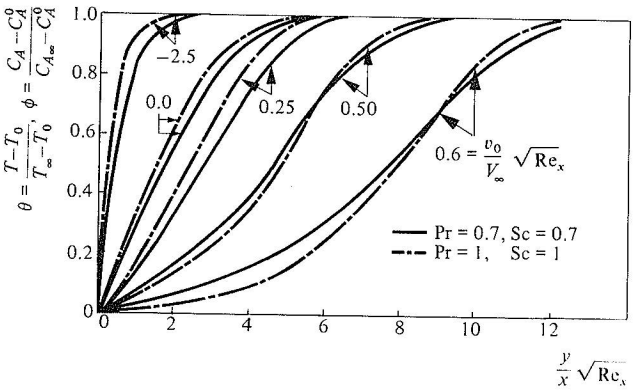

Fig. 15.6 Temperature and concentration profiles in a laminar boundary layer on a flat plate for Pr = Sc = 0.7, and Pr = Sc = 1. Curves for Pr = Sc = 1 also represent velocity profiles. (From J. P. Hartnett and E. R. G. Eckert, *Trans. ASME* **79**, 247 (1957).)

These profiles show a dependence on the mass flux ($v_0\sqrt{\mathrm{Re}_x}/V_\infty$). Mass transfer away from the plate (positive v_0) gives flatter profiles as would be true if the solid surface were porous and a gas diffused upward through the plate, or if a liquid passed through the porous plate and evaporated. On the other hand, mass transfer towards the plate (negative v_0) gives steeper profiles; this situation can be obtained if condensation occurs at the surface, or suction is applied to a porous

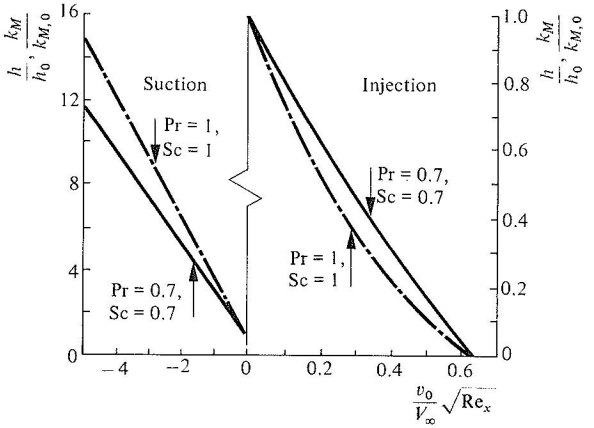

Fig. 15.7 Heat- and mass-transfer coefficients for laminar flow over a flat plate. Subscript zero indicates the respective coefficients for zero bulk flow normal to wall. (From J. P. Hartnett and E. R. G. Eckert, *ibid.*)

plate. Figure 15.7 shows the local heat- and mass-transfer coefficients plotted against the parameter $v_0\sqrt{\mathrm{Re}_x}/V_\infty$. For $v_0 = 0$ (no mass transfer, or, more realistically, at low mass-transfer rates), the local mass-transfer coefficient is given by Eq. (7.26) with a simple change of notation, namely:

$$h_x \to k_{M,x},$$

$$k \to D_A,$$

$$\mathrm{Pr} \to \mathrm{Sc}.$$

Then, the local Sherwood number is

$$\mathrm{Sh}_x = 0.332\,\mathrm{Sc}^{0.343}\,\mathrm{Re}_x^{1/2}, \tag{15.91}$$

and the average Sherwood number

$$\mathrm{Sh}_L = 0.664\,\mathrm{Sc}^{0.343}\,\mathrm{Re}_L^{1/2}. \tag{15.92}$$

15.8 CORRELATIONS OF MASS-TRANSFER COEFFICIENTS FOR TURBULENT FLOW

We have seen in the previous sections that many forced-convection mass-transfer situations are completely analogous to heat-transfer situations, and the appropriate heat-transfer solutions apply with simple changes of notation, namely:

$$\alpha \to D_A,$$

$$T \to C_A,$$

$$\mathrm{Pr} \to \mathrm{Sc},$$

$$\mathrm{Nu} \to \mathrm{Sh}.$$

In addition, we may assume that the results for natural convection resulting from density differences caused by mass transfer may be correlated by a mass-transfer Grashof number,

$$\mathrm{Gr}_M = g\xi(X_A - X_{A\infty})L^3/\nu^3,$$

where ξ is the concentration coefficient of volumetric expansion defined as:

$$\xi = \frac{1}{\rho}\left(\frac{\partial \rho}{\partial X_A}\right)_T.$$

In this case, we may use correlations for heat transfer to yield mass-transfer data if the substitution

$$\mathrm{Gr} \rightarrow \mathrm{Gr}_M$$

is made. The flow parameters such as Re and position parameters such as L/D remain the same.

We noted in Chapter 8 that in turbulent flow there is a parallel between the friction factor f for turbulent flow in tubes and heat transfer, in terms of a quantity known as the Chilton–Colburn "j-factor", j_H:

$$j_H = \frac{\mathrm{Nu}}{\mathrm{RePr}}(\mathrm{Pr})^{2/3} = \frac{f}{2}. \tag{8.6}$$

Continuing the analogy, we define a mass-transfer j-factor, j_M, for fully developed flow in round tubes:

$$j_M = \frac{\mathrm{Sh}}{\mathrm{ReSc}}(\mathrm{Sc})^{2/3} = \frac{f}{2}. \tag{15.93}$$

If flow is not fully developed, we use Fig. 8.2 where we take L/D into account, and substitute j_M for j_H. Epstein[2] used Eq. (15.93) to compute the corrosion rate of an iron tube by molten mercury; apparently, the mass transfer of iron into the mercury stream determines the rate of this process.

In the case of flow past a flat plate, from the results of Chapter 8, we write for average values in *laminar* flow:

$$j_H = j_M = \frac{f}{2} = \frac{0.664}{\sqrt{\mathrm{Re}_L}}, \tag{15.94}$$

and in *turbulent* flow

$$j_H = j_M = \frac{f}{2} = \frac{0.037}{(\mathrm{Re}_L)^{0.2}}. \tag{15.95}$$

[2] L. F. Epstein, *Chem. Engr. Progress Symposium Series* **53**, No. 20, 67.

This relationship has been found to adequately describe the rate of deposition of metallic solutes from liquid to solid,[3] and the rate of dissolution of carbon into iron melts.[4]

In flow around curved surfaces, such as spheres and cylinders, $f/2$ greatly exceeds j_H and j_M. However, the analogy still holds between heat and mass transfer, so that j_H and j_M should be equivalent. To illustrate this, consider the heat-transfer correlation given in Chapter 8 for forced convection around a sphere of radius R:

$$2hR/k_f = 2.0 + 0.60\,\mathrm{Re}_f^{1/2}\,\mathrm{Pr}_f^{1/3}. \tag{8.10}$$

Translated into the j_H form it becomes

$$j_H = \frac{2.0}{\mathrm{RePr}^{1/3}} + \frac{0.60}{\mathrm{Re}^{1/2}}.$$

By analogy we get

$$j_M = \frac{2.0}{\mathrm{ReSc}^{1/3}} + \frac{0.6}{\mathrm{Re}^{1/2}}. \tag{15.96}$$

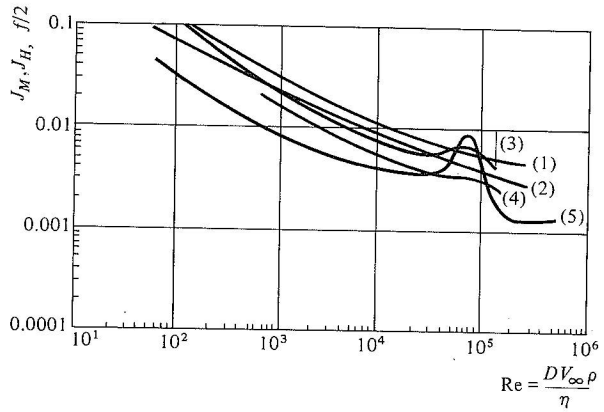

Fig. 15.8 Comparison of mass-, heat-, and momentum-transfer to spheres. (1) $f/2$; (2) Chilton–Colburn factor j_H; (3) j_M for cinnamic acid–water system; (4) j_M for 2-naphthol–water system; (5) j_M for uranium dissolving in cadmium. (Data from E. D. Taylor, L. Burris, and C. J. Geankoplis, *I. & E. C. Fundamentals* **4**, 119 (1965); and T. R. Johnson, R. D. Pierce, and W. J. Walsh, *ANL Report on Contract W-31-109-eng-38*, 1966.)

Figure 15.8 illustrates the results of experiments where j_M is plotted as a function of Re for dissolution of uranium spheres in flowing cadmium[5], cinnamic

[3] W. N. Gill, R. P. Vanek, R. V. Jelinek, and C. S. Grove, *AIChEJ* **6**, 139 (1960).
[4] M. Kosaka and S. Minowa, *Trans. Japan Iron and Steel Inst.* **8**, 393 (1968).
[5] F. D. Taylor, L. Burris, and C. J. Geankoplis, *I. & E.C. Fundamentals* **4**, 119 (1965).

acid spheres in flowing water, 2-naphthol spheres in flowing water[6], and for comparison purposes, j_H[7], and $f/2$[8]. Note that the data from the liquid metal experiments show lower values of j_M at low Re values than those observed in the organic system experiments. This may be partially corrected for by the presence of the Schmidt number in the expression given in Eq. (15.96), which is not plotted in Fig. 15.8. No equation accounts for the peak in j_M near Reynolds numbers of 10^5, so usually the graph is preferred rather than an equation in this range.

For natural convection, the mass transfer analog of

$$\mathrm{Nu}_L = 0.13\,(\mathrm{Gr}_L\mathrm{Pr})^{1/3} \tag{8.18}$$

has been applied to both the rate of dissolution of carbon in molten iron[9] and the rate of dissolution of steel in molten iron–carbon alloys[10], and found to be quite reasonable as an approximation, with the best fit of the data yielding the equation

$$\mathrm{Sh}_L = 0.11\,(\mathrm{Gr}_{M,L}\mathrm{Sc})^{1/3}. \tag{15.97}$$

Many metallurgical processes depend on gas–liquid contact and mass transfer between the phases. Although this is a very complex area,[11] several relationships have been found that describe the process of mass transfer *on the liquid side* of a gas bubble–liquid interface. One of the most useful is that of Hughmark.[12] His expression is

$$\frac{k_M d}{D} = 2.0 + a\left[\left(\frac{V_t d}{\nu}\right)^{0.48}\left(\frac{\nu}{D}\right)^{0.339}\left(\frac{g^{1/3}d}{D^{2/3}}\right)^{0.072}\right]^b, \tag{15.98}$$

where d is the bubble diameter, V_t is the terminal velocity of the rising bubble, and a and b are constants that depend on whether the bubbles act singly or in swarms. For single bubbles, $a = 0.061$ and $b = 1.61$. This relationship has been tested in molten copper–carbon monoxide systems, and was found satisfactory for describing the rate of transfer of oxygen in the copper to the interface.[13]

Note that the Chilton-Colburn analogy is applicable only at relatively low mass-transfer rates, and that the best analogous results are obtained when similar materials are utilized in both the heat- and analogous mass-transfer situations. Turbulent flow mass-transfer correlations based on studies using common liquids appear to be directly translatable into liquid metal systems, but heat transfer

[6] L. R. Steele and C. J. Geankoplis, *AIChEJ* **5**, 178 (1959).
[7] T. K. Sherwood, *Ind. Engr. Chem.* **42**, 2077 (1950).
[8] F. H. Garner and R. D. Suckling, *AIChEJ* **4**, 114 (1958).
[9] M. Kosaka and S. Minowa, *ibid.*
[10] M. Kosaka and S. Minowa, *Tetsu-to-Hagane* **53**, 983 (1967).
[11] For reviews, see P. H. Calderbank, *Trans. Inst. Chem. Engrs.* **212**, 209 (1967); F. H. H. Valentin, *Absorption in Gas–Liquid Dispersions*, Spon Ltd, London, 1967.
[12] G. A. Hughmark, *I. & E. C. Process Design and Development* **6**, 218 (1967).
[13] C. R. Nanda and G. H. Geiger, *Metallurgical Transactions* **2**, 1101 (1971).

data are not quite as accurate in predicting mass transfer, although usually satisfactory to within an order of magnitude.

Also, many of the tests of applicability of heat transfer correlations to mass transfer involving the gas phase have not been made at conditions likely to be of interest to metallurgists, particularly at elevated temperatures and high rates of transfer, so they should be used with caution.

Example 15.4 Graphite particles are often added to molten cast iron in order to increase the carbon content when scrap steel is used as starting material. The time required to dissolve the particles is of interest. Determine the time to dissolve particles of graphite as a function of the bath's carbon content.

The particles have a shape factor λ of 1.5, and a characteristic dimension $\bar{D}_p$ of 0.14 cm. The particles float, and are swept to the side of the surface of the melt by the magnetically induced stirring action resulting in a relative metal velocity of approximately 25 cm/sec. Due to the displacement of metal by graphite, the surface area of an individual particle in contact with the metal is calculated as $\frac{3}{8}$ of the total particle surface area. In addition, a portion of the particle exposed to the atmosphere is burned to CO due to the air circulating over the bath surface. Thus the recovery of carbon in the melt is less than 100%, and experience shows that, in fact, the recovery is only 50%. Therefore, the mass of an individual particle (of density ρ_s) that dissolves in the melt is

$$m = \frac{1}{2}\left(\frac{\pi}{6}\bar{D}_p{}^3\rho_s\right),$$

and its surface area exposed to the melt is

$$A = \tfrac{3}{8}\pi\bar{D}_p{}^2\lambda.$$

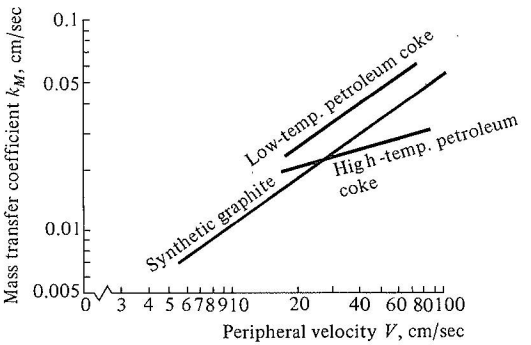

Fig. 15.9 Mass-transfer coefficients for carbon dissolution in Fe–C melts. (From R. G. Olsson, V. Koump, and T. F. Perzak, *Trans. AIME* **236**, 426 (1965); O. Angeles, G. H. Geiger, and C. R. Loper, *Trans. AFS* **76**, 629 (1968); and M. Kosaka and S. Minowa, *Trans. Japan Iron Steel Inst.* **8**, 393 (1968).)

Solution. The mass flow, in terms of g C/sec, is

$$\frac{dm}{dt} = -k_M A \rho_L (C_0 - C_\infty),$$

where ρ_L is liquid density, g/cm^3, C_0 is weight fraction of carbon at the particle melt interface, and C_∞ = weight fraction of carbon in the bulk melt.

We evaluate the mass-transfer coefficient from Fig. 15.9 which has been developed by several investigators for the dissolution of rotating carbon rods in Fe–C melts. For a velocity of 25 cm/sec, k_M for graphite is 0.02 cm/sec. Now, since

$$\frac{dm}{dt} = -\tfrac{1}{4}\pi \bar{D}_p^2 \rho_s \frac{d\bar{D}_p}{dt},$$

and the area is as given above, we can determine the time to dissolve a particle:

$$\int_{\bar{D}_p}^{0} d\bar{D}_p = \tfrac{3}{2} k_M \lambda \frac{\rho_L}{\rho_s}(C_0 - C_\infty) \int_0^t dt,$$

or

$$t = \frac{2\rho_s \bar{D}_p}{3\rho_L \lambda k_M (C_0 - C_\infty)}, \text{ sec.}$$

The results are plotted below.

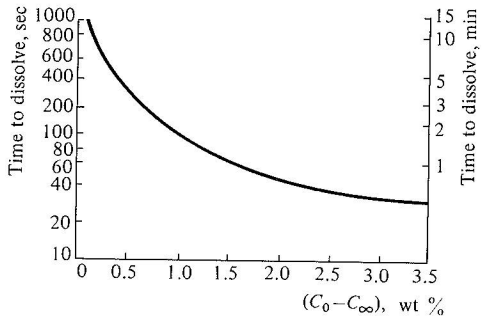

15.9 MODELS OF THE MASS-TRANSFER COEFFICIENT

Since most conditions in which mass transfer is important involve fluids undergoing turbulent motion, we must usually rely on the preceding correlations, with experimental studies giving the necessary empirical coefficients. However, there are many situations to which these test data do not directly apply, such as beyond the experimental scope of variables, and it is desirable to know whether and how

the experimental data can be extended to the new situation. Several theories of the process of mass-transfer have been developed, and they attempt to present models of what actually happens at the interface between two fluids or between a fluid and solid from a fundamental viewpoint, in order to aid in intelligent extrapolation of data.

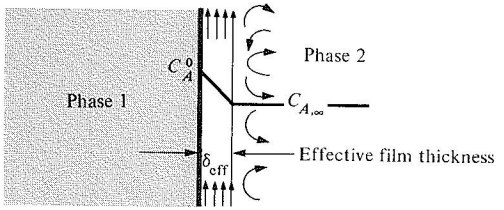

Fig. 15.10 The "effective film thickness" model.

The oldest theory is the film theory of Lewis and Whitman[14] who suggested that there is an unmixed layer or film in the fluid next to the actual interface, continuously exposed to the completely mixed bulk fluid on one side and to the other phase on the other. This layer, devoid of any fluid motion, is supposed to offer all the resistance to the transfer of component A from the interface into the bulk solution, as depicted in Fig. 15.10. The transfer takes place purely by atomic or molecular diffusion through the film. Figure 15.10 indicates the concentration profile assumed in the model. Since the entire concentration change from $C_{A\infty}$ to C_A^0 is assumed to take place within the film in a steady-state manner, and since the mass-transfer coefficient is defined by

$$j_A = k_M (C_A^0 - C_{A\infty}),$$

we can compare this to

$$j_A = -D\frac{dC_A}{dx} = +D\frac{(C_A^0 - C_{A\infty})}{\delta_{\text{eff}}},$$

with the result that $k_M = D/\delta_{\text{eff}}$, where δ_{eff} is the effective film thickness. This result often appears in the metallurgical literature in cases where the flux is measured and the overall concentration change $(C_A^0 - C_{A\infty})$ is known, and then either the diffusivity is known (or more often assumed) and δ_{eff} is calculated, or *vice versa.* As noted below, the significance of δ_{eff} is dubious, at best.

From a fluid mechanics standpoint, it was recognized at an early stage that interfaces between fluids are bound to be unstable with time, and that any given element of fluid at the interface does not remain there for long. Thus, the film

[14] W. K. Lewis and W. Whitman, *Ind. Engr. Chem.* **16**, 1215 (1924).

theory is much too crude to be really meaningful. Higbie[15] proposed a model to describe the contact between two fluids, in which he assumed that one fluid exposes a "particle" of fluid to the other phase for an average time θ, which is taken to be extremely short, such that the particle is subject only to unsteady-state diffusion or "penetration" by the transferred species during its contact time with the other phase. The particle is assumed to be stagnant internally during this time, and well mixed before and after. Figure 15.11 gives a schematic picture of the situation. This theory results in a prediction that

$$k_M = 2\sqrt{\frac{D}{\pi\theta}}. \tag{15.99}$$

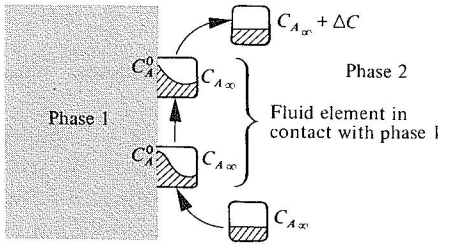

Fig. 15.11 Schematic diagram of fluid motion in penetration theory.

The logical extension of this theory was performed by Danckwerts[16] who suggested that the idea of a constant time of exposure θ ought to be replaced by an average time of exposure calculated from an assumed distribution of residence times of the "particles" at the surface. The result is again a relationship of the form

$$k_M \propto \sqrt{D}. \tag{15.100}$$

The constants in his equation, like the constant θ in Higbie's equation, are not readily obtainable, with the exception of bubbles rising through a liquid in which case we may estimate θ to be the time required for a bubble to rise a distance equal to its diameter.

When considering the two theories, it is apparent that the dependence of k_M on D is different. Experimentally, it has been found that k_M is proportional to D^n where n varies from 0.5 to 1.0, depending on the fluids and the circumstances. In order to resolve this discrepancy, Dobbins[17] and Toor and Marchello[18] proposed a combined *film penetration theory* in which the residence time of the surface

[15] R. Higbie, *Trans. AIChEJ* **31**, 365 (1935).
[16] P. U. Danckwerts, *Ind. Engr. Chem.* **43**, 1460 (1951).
[17] W. E. Dobbins, *Int. Conference on Water Pollution Research*, London, 1962, Pergamon Press, New York, 1964, page 61.
[18] H. L. Toor and J. M. Marchello, *AIChEJ* **4**, 97 (1958).

elements (Higbie model) is long enough to allow the concentration gradient to approach steady-state across the finite thickness of the element (film model). This theory approaches each of the other theories as limiting cases. When D is large or the rate of surface renewal is small (θ is large), then n approaches 1.0 and so the film theory is applicable. When D is small or θ is small (rapid surface renewal rate), n approaches 0.5, and the penetration theory results. In any case, there are still parameters that must be specified in order to use the theory for predictive purposes, and they are not readily obtainable.

PROBLEMS

15.1 At 1000°F metal A is soluble in liquid B but B is not soluble in solid A as shown below in the pertinent part of the phase diagram.

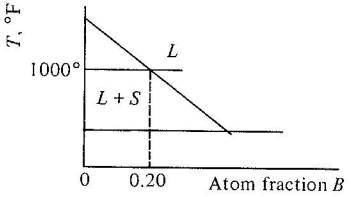

A 2-in. diameter cylinder of A is rotated at 1000 rpm in a large melt of 0.5 atom fraction B at 1000°F, and it is noted that after 15 min the bar diameter is 1.90 in. For the same temperature, estimate the bar diameter after 15 min if another 2-in. diameter cylinder of A is rotated in a large melt of 0.25 atom fraction B. We can assume that the molar volume of liquid A–B alloys is constant.

15.2 Use dimensional analysis to show

a) $\mathrm{Sh} = f(\mathrm{Re}, \mathrm{Sc})$ for forced convection;
b) $\mathrm{Sh} = f(\mathrm{Gr}, \mathrm{Sc})$ for natural convection.

15.3 Levitation melting is a means of supporting a metallic melt by an electromagnetic field. No impurities are added in melting and operation under an inert atmosphere removes dissolved gases. At 3000°F and 1 atm hydrogen pressure, the solubility of hydrogen in iron is 31 cm^3 per 100 g of iron. Estimate the rate at which hydrogen can be removed from a levitated drop of iron that initially contains 10 ppm in the set-up shown below. Assume that no convection occurs within the iron drop.

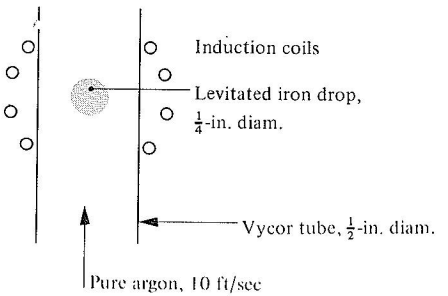

15.4 Derive expressions for diffusion through a spherical shell that are analogous to Eq. 15.12 (concentration profile) and Eq. 15.14 (molar flux).

15.5 Hydrogen gas is being absorbed from a gas in an experimental set-up shown in the figure below. The absorbing liquid is aluminum at 1400°F which is falling in laminar flow with an average velocity of 6 in. per min.

What is the hydrogen content of the aluminum leaving the tube if it enters with no hydrogen? Assume that at $T = 1400$°F, and 1 atm hydrogen pressure, the solubility of hydrogen is 1 cm^3 per 100 g of aluminum, the density of Al = 2.5 g/cm^3, and $D_H = 1 \times 10^{-5}$ cm^2 sec^{-1}

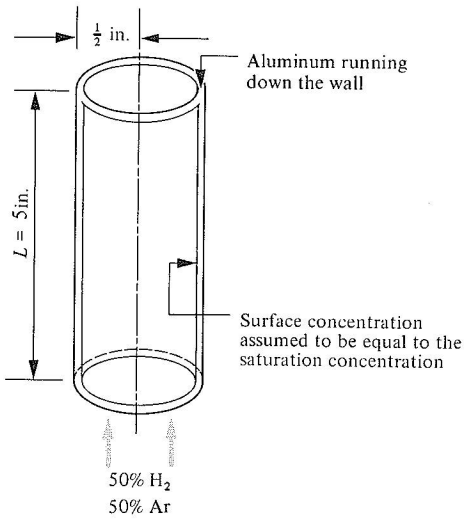

16

INTERPHASE MASS TRANSFER

In Chapter 15 we undertook much of the analytical presentation to familiarize ourselves with mass-transfer coefficients as they arise from considerations of diffusion with convection in a single phase only. There are many situations, however, in which two fluids or a solid and fluid are in contact, and interphase transfer by diffusion with convection takes place in one or both phases. In some cases, convective mass transfer may be important in controlling the overall rate; in others it is not important. If there is a reaction at the interface, it may very well be the controlling step.

Experimentally, it is difficult to study interphase transfer, and at the same time separate the individual phase resistances; so an *overall transfer coefficient* is usually measured. Having determined this coefficient, we then attempt, via a mathematical model, to *deduce* the individual phase coefficients, such as those presented in Chapter 15. In some cases the results are clear cut, and we are then able to adjust process conditions to optimize the process. However, in other cases, we cannot differentiate between models even though they may be based on important differences in basic assumptions, because their predictions can be numerically similar within experimental error. Then, we deal with the overall coefficients and utilize them, but only if the fluid conditions are similar in both the prototype and model cases.

The objective of this chapter is to indicate the relationships between the individual phase transfer coefficients and the overall coefficients, and to examine several cases in detail, showing how different fluid conditions can influence the overall coefficient through their effect on the individual coefficients.

16.1 TWO-RESISTANCE MASS-TRANSFER THEORY

Let us investigate the situation as it might exist in a gas–liquid physical reaction. Figure 16.1 depicts the phases in contact and the concentration profiles in each phase. The *mole fraction* of A in the bulk gas phase is $Y_{A\infty}$, and it decreases to Y_A^* at the interface. In the liquid, the mole fraction drops from X_A^* at the interface to $X_{A\infty}$ in the bulk liquid. The bulk concentrations $X_{A\infty}$ and $Y_{A\infty}$ are obviously not in equilibrium, otherwise diffusion of the solute would not occur. To determine